Appl. Phys. B (2015) 119:153–164
DOI 10.1007/s00340-015-6069-1

Applied Physics B
Lasers and Optics

Low-power, open-path mobile sensing platform for high-resolution measurements of greenhouse gases and air pollutants

Lei Tao · Kang Sun · David J. Miller · Dan Pan · Levi M. Golston · Mark A. Zondlo

Received: 3 November 2014 / Accepted: 25 February 2015 / Published online: 10 March 2015

Abstract A low-power mobile sensing platform has been developed with multiple open-path gas sensors to measure the ambient concentrations of greenhouse gases and air pollutants with high temporal and spatial resolutions over extensive spatial domains. The sensing system consists of four trace gas sensors including two custom quantum cascade laser-based open-path sensors and two LICOR open-path sensors to measure CO_2, CO, CH_4, N_2O, NH_3, and H_2O mixing ratios simultaneously at 10 Hz. In addition, sensors for meteorological and geolocation data are incorporated into the system. The system is powered by car batteries with a low total power consumption (~200 W) and is easily transportable due to its low total mass (35 kg). Multiple measures have been taken to ensure robust performance of the custom, open-path sensors located on top of the vehicle where the optics are exposed to the harsh on-road environment. The mobile sensing system has been integrated and installed on top of common passenger vehicles and participated in extensive field campaigns (>400 h on-road time with >18,000 km total distance) in both the USA and China. The simultaneous detection of multiple trace gas species makes the mobile sensing platform a unique and powerful tool to identify and quantify different emission sources through mobile mapping.

L. Tao (✉) · K. Sun · D. J. Miller · D. Pan · L. M. Golston · M. A. Zondlo
Department of Civil and Environmental Engineering, Princeton University, Princeton, NJ 08544, USA
e-mail: ltao@princeton.edu

L. Tao · K. Sun · D. J. Miller · D. Pan · L. M. Golston · M. A. Zondlo
Center for Mid-Infrared Technologies for Health and the Environment, NSF-ERC, Princeton, NJ 08544, USA

Present Address:
D. J. Miller
Institute at Brown for Environment and Society, Brown University, Providence, RI 02912, USA

1 Introduction

In recent years, vehicle-based mobile sensing laboratories have been developed and used extensively for the environmental studies [1–9]. The ground-based, mobile sensing platforms measure pollutants and greenhouse gases on local to regional scales at high spatiotemporal resolution [2–9]. A mobile laboratory is advantageous in that it addresses the spatial undersampling problems common to traditional stationary monitoring stations. Mobile measurements provide comprehensive source attribution of greenhouse gases and air pollutants and information on their distribution, particularly for short-lived trace gas species that show high spatial variability.

Laser-based, trace gas detection is used in many mobile laboratories due to its high sensitivity, selectivity, and fast time response [3]. Tunable diode laser absorption spectroscopy (TDLAS) is a general technique for the analytical instruments used in the environmental studies to monitor atmospheric trace gas species. In order to achieve high sensitivity and selectivity, TDLAS measurements are generally performed with long optical pathlengths in enclosed optical cells that are regulated at low pressures (~1–50 hPa). The selected optical absorption lines are narrow with little or no interferences from neighboring absorption lines of other trace gas species [10]. A closed-path approach, however, poses sampling problems for the species such as water vapor (H_2O) and ammonia (NH_3) that readily adsorb and desorb from the instrument surfaces (e.g., inlets, tubing, and optical cells). To improve the response time, a high

flow rate is needed to equilibrate the surfaces faster, but this requires large, heavy, and power hungry pumps. Even with a high pumping speed and sophisticated inlet design, sensor response is still a substantial challenge for the sticky gases like NH_3. Furthermore, even gases without sampling issues such as N_2O require large pumps to achieve fast time response (10 Hz). To meet the high power consumption of the onboard sensors and their support systems (e.g., pumps, instrument racks and air conditioning), existing mobile sensing platforms [3, 5–9] are typically deployed on heavily modified vans or trucks and are powered by portable generators or large battery units.

Open-path TDLAS techniques do not require a pressure-regulated closed cell nor their associated pumping systems. Ambient air passes freely through the optical cell, and thus, the sensors are capable of high time resolution, fast response time, and lower sampling artifacts than closed-path systems [11–14]. However, there are many challenges to measure the trace gases directly under the ambient conditions including spectral interferences, pressure broadening of lineshapes, deterioration of any exposed optics, and a wide range of environmental conditions (e.g., precipitation, road spray, dust, insects, extreme temperatures).

Individual laser-based, open-path sensors have been previously developed to detect atmospheric carbon monoxide (CO, a tracer for fossil fuel combustion), nitrous oxide [N_2O, an important greenhouse gas (GHG) and a major ozone depleting substance; 13], NH_3 [a gas phase precursor for fine aerosol; 14], and CH_4 [a potent greenhouse gas; 17]. The N_2O, CO, and NH_3 measurements take advantage of the gas molecules' fundamental absorption bands in the mid-infrared at 4.54 μm (for N_2O/CO) and 9.06 μm (for NH_3) by using quantum cascade lasers (QCL) for high-sensitivity detection. The targeted absorption lines in the mid-infrared are specially selected to minimize spectral interferences from neighboring atmospheric species at ambient pressure while also to maintain relatively strong linestrengths (within a factor of two of the strongest ones in the fundamental bands). The most significant interferences are water vapor, though other trace gases need to be considered depending upon the wavelength of interest and precision, accuracy, and detection limit needed. Both of the QCL-based sensors in the mobile laboratory have been extensively tested in the field [15, 16].

This paper reports the development and the field deployment of the first open-path, multiple trace gas mobile sensing platform. By integrating individual open-path sensors, this platform detects the four most important greenhouse gases (CO_2, CH_4, N_2O, and H_2O) and two key air pollutants (NH_3, CO) simultaneously at 10 Hz. It provides a lightweight, compact and low-power alternative to the closed-path sensors and also allows for unprecedented time response for the sticky gas such as NH_3. The simultaneous detection of the six different gases provides a powerful tool to fingerprint different emission sources and quantify their emissions. The mobile platform has been field deployed for 18,000 km of on-road measurements in five different field experiments in the USA and China. This study describes additional modifications to incorporate the sensors into the mobile system and demonstrates its field performance and measurement results for distinguishing and characterizing trace gas sources in urban areas.

2 Material and methods

2.1 Onboard sensors

The mobile platform has four open-path optical gas sensors: QCL NH_3 sensor [14], QCL CO/N_2O sensor [13], LI-COR LI-7500A CO_2/H_2O sensor, and LI-7700 CH_4 sensor [17]. A portable weather station (Vaisala WXT520) provides the necessary meteorological parameters (temperature, pressure, humidity, wind speed/direction, and precipitation rate). Figure 1 shows a photograph of the mobile system during a field campaign in Beijing, China, in June 2013. Although the individual QCL sensors have been demonstrated previously [13, 14], multiple revisions to the original designs have been made in order to make them more robust onboard a mobile platform. As a result, the sensor configurations varied and evolved during different field campaigns, and this study will present the most optimal configurations to date and rationale for their design when changes from the original studies were significant.

The specifications of the trace gas sensors are shown in Table 1. The LI-7500A is a non-dispersive infrared (NDIR) sensor, which measured the broadband absorption of H_2O and CO_2 simultaneously at high sampling frequency [18]. The LI-7700 and two custom QCL-based sensors used wavelength modulation spectroscopy (WMS). WMS is a widely applied technique for sensitive measurement

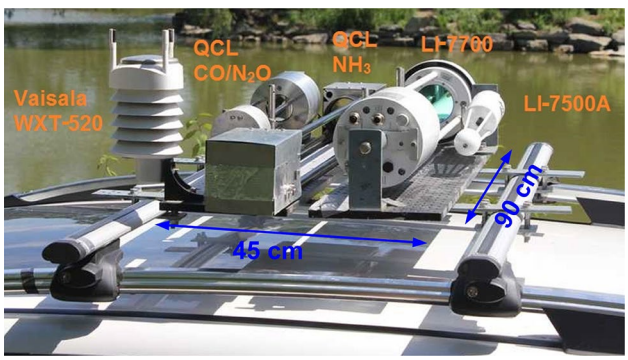

Fig. 1 Mobile platform on top of a passenger vehicle in Beijing, China

Table 1 Specifications of four sensors

Sensor	Light sources	Sensitivity at 10 Hz	Optical pathlength	Power requirement	Sensor head mass
QCL NH_3	9.06 µm QCL	150 pptv NH_3	46 m	45 W	6.8 kg
QCL CO/N_2O	4.54 µm QCL	3 ppbv CO 0.2 ppbv N_2O	15.8 m	45 W	5.4 kg
LI-7500A	IR Lamp	0.11 ppmv CO_2 0.0047 ppmv H_2O	0.125 m	12 W	0.75 kg
LI-7700	1.65 µm VCSEL	5 ppbv CH_4	30 m	8 W	5.2 kg

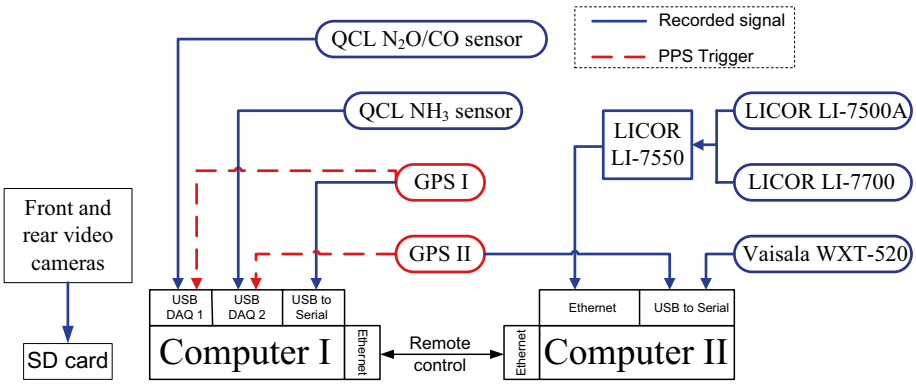

Fig. 2 Schematic of the mobile platform

of trace gas species [19]. Its basic approach is similar to direct absorption spectroscopy but with an additional fast (10 s of kHz) sinusoidal modulation applied to the laser current (wavelength) that is scanned in a sawtooth waveform across an absorption line at ~0.1–1 kHz. The modulated absorption signal on the photodetector was processed through a lock-in amplifier which demodulated the signal at the fundamental modulation frequency and its integral multiples (harmonics). In this way, WMS shifted the detection bandwidth to a higher frequency that rejected low-frequency noise (e.g., 1/f laser noise) in order to improve the sensitivity. Harmonic spectra of the photodiode signals were intrinsically dependent on the spectral parameters and the gas properties. The 2nd harmonic signal was generally used to retrieve the gas concentration. Ideally, WMS is a baseline free technique compared to direct absorption spectroscopy, which requires complicated algorithms to remove baselines, especially for pressure-broadened features. WMS is one of the most precise and appropriate techniques for probing air-broadened and overlapping absorption features in open-path sensors.

2.2 Mobile platform

The optical sensor heads in the mobile platform were mounted close to each other in parallel on two slim (90 cm in length, 20 cm in width and 1.27 cm in thickness, Thorlabs, Inc., USA) aluminum optical breadboards, which in turn were mounted onto a commercial roof rack (Thule 400) of a passenger car as shown in Fig. 1. Vibration damping rubber mounts were placed between the breadboard and roof rack to isolate vibrations from the road. The control units for the sensors were placed in the backseat or the trunk of the vehicle with the cables running through either the windows or sunroof. The base of the optical sensing system was able to be mounted on different common passenger vehicles using commercially available standard luggage or ski racks, allowing great flexibility to use rental vehicles for different field campaigns. Chevy Impalas (2013, 2014 models) and Honda CRVs (2013, 2014 models) have been used to host the sensor system. The maximum load for the roof rack was 75 kg. The total mass mounted on top of the vehicle was 35 kg. The compact size and modular structure of the system allowed it to be packed conveniently in checked airline luggage for the overseas deployment and also minimized customs/shipping issues compared to the international freight shipments.

A schematic of the mobile platform is shown in Fig. 2. Two computers were used to control the sensors and collect the data. Computer I was a laptop computer that controlled both QCL sensors as well as computer II through remote access. The computer II was a low-power single-board computer that recorded the data from the Vaisala weather transmitter and from the LICOR sensors via the LI-7550 interface unit. The two QCL sensors were triggered by pulse-per-second (PPS) signals from the Global Positioning System (GPS, MTK3339). To ensure proper triggering of the QCL sensors in places where the GPS signal

was blocked (e.g., tunnels), the GPS receivers (MTK3339) were flashed with firmware to provide the PPS signal at all times. Both computers recorded the GPS output for synchronization of the timestamp and the location information. A custom LabVIEW-based software was used for the sensor control and data logging. Front and rear video cameras were equipped inside the vehicle to record on-road videos into a SD (Secure Digital) memory card for further analyses. The Vaisala WXT520 weather transmitter measured 2D wind speeds at 5 Hz using ultrasonic transducers on a horizontal plane (data averaged to 1 Hz for analyses). It was mounted with its north aligned to the forward direction of the car. The wind speed vector was calculated as the difference between the velocity vector measured by Vaisala and the velocity vector of the car as derived from sequential GPS readings [20]. The accuracy of 1 Hz GPS-derived vehicle velocities when used in differential GPS mode was 0.1 knot (~0.05 m s^{-1}) within the USA (worse by a factor of two in China where differential GPS was not available). The stated accuracy of the Vaisala WXT520 weather station is ±3 % at 10 m s^{-1} and ±3° in direction. The combined accuracy of the derived wind velocity measurement had a 1 Hz accuracy of ±5 % in wind speed and ±5° in wind direction at a vehicle speed of 10 m s^{-1}.

The entire mobile sensor system—computers and sensors—consumed ~200 W. The computer I and the cameras were powered directly from common 12 VDC car outlets. The rest of the components were powered by two 12 V car batteries (90 A h) placed in the back of the vehicle. The system operated for as long as 14 h without recharging the batteries, and this duration of time is typically longer than 1 day's worth of sampling. The mobile system was deployed at speeds as high as the legal speed limit (33.5 m s^{-1}) with no noticeable change in performance, thereby providing large spatial coverage in addition to high-resolution measurements.

2.3 Optomechanical optimization

A major challenge for the open-path, mobile sensing system was to maintain the integrity of the optomechanical design for robust on-road performance. The two QCL sensors and LI-7700 all used open-path, multiple pass optical cells to achieve long optical pathlengths in a relatively short mirror separation. The structural robustness of the optical cell and its associated components were critical for maintaining the optical alignment in the high airspeeds and vibrations of a vehicle. A standard Herriott cell formed by two spherical mirrors [21] was used in the LI-7700 to achieve a 30 m pathlength with 47 cm mirror separation [17]. For the QCL sensors, an astigmatic open-path multipass cell consisting of two cylindrical mirrors [22] was originally tested in the field. However, sufficiently tight tolerances on mirror separation, rotational angle, and input laser beam angle [23] were not successfully maintained in the field. Significant changes in alignment were observed over the course of a diurnal temperature cycle (13 °C). Instead, a standard Herriott cell design was used in both QCL sensors that allowed for more tolerance in the optical alignment. The NH_3 sensor had an optical cell with two 76-mm-diameter mirrors separated by ~52 cm to get a 46 m pathlength. The N_2O/CO sensor uses two 51-mm-diameter mirrors with a ~28 cm separation for a 15.8 m pathlength. With the structural reinforcement of the carbon fiber rods, the Herriott optical cells maintained the optical alignment and the structural rigidity in the field conditions on the rooftop of a moving vehicle.

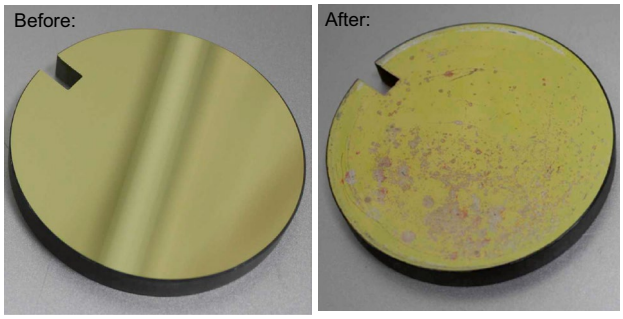

Fig. 3 Comparison of protected silver-coated mirror before and after a three-week field campaign

The potential for deterioration of exposed optics was an unavoidable drawback of the open-path mirror configuration for long-term deployment of the system. The multipass mirrors were the most significantly exposed optics due to the open-path nature of the sampling. When on top of a vehicle for mobile sampling, these mirrors experienced rain, dew, frost, dust, road spray, and insect impaction events. As a result, the mirrors needed to be kept relatively clean to maintain the surface reflectivity. In the LI-7700, two dielectric-coated mirrors for near-infrared light at 1.65 μm maintained good surface quality and high reflectivity under frequent (2–4 times per day) cleaning. Dielectric-coated mirrors with high-reflectivity (>98 %) for the mid-infrared spectral region for the QCL-based sensors were not investigated due to their expected low durability due to the need for thicker coating layers than in the near-IR. Instead, protected silver-coated mirrors were first tested for both mid-infrared sensors. Figure 3 shows a protected silver-coated mirror before and after a three-week field campaign and 3,000 km of on-road measurements in China. Note that the protective coating gave the mirrors a golden color. The dielectric overcoat that helped to protect the silver [24] showed evidence of pitting and degradation. At the end of the campaign, the maximum intensity of the detector signal after mirror cleaning dropped to ~10 % of

the original value when the mirrors were new. The high reflectivity of silver degraded quickly due to corrosion [25] once it was exposed to the atmosphere. Furthermore, silver has poor adhesion to most substrates, which resulted in significant physical damage from impaction events during the field experiment. Note that protected silver-coated mirrors from four different vendors were used and showed comparable performance.

To address the mirror durability problem, polished uncoated molybdenum (Mo) mirrors were ultimately used instead of protected silver-coated mirrors for the Herriott cells of the mid-infrared sensors. Mo mirrors have been used for guiding high-power mid-IR lasers in harsh industrial environments. With advanced polishing techniques, a high-quality (scratch/dig of 60–40, front surface flatness of λ/4 at 632 nm) uncoated Mo mirror (Rocky Mountain Instrument Co., USA) was able to achieve a high natural broadband reflectivity of >98 % from 4 to 12 μm. The Mo mirror surface withstood frequent cleaning and resisted organic solvents and detergents. The Mo mirrors have shown great performance with almost no deterioration in the reflectivity and the surface quality. The detector light intensity of the NH_3 sensor equipped with Mo mirrors has remained within 10 % of the original level after more than 10,000 km of on-road measurements.

2.4 Power consumption and thermal management

The power consumption of a mobile platform directly influences its design and the performance of the system. Generally, a mobile platform with a high power consumption requires a bulky and complicated system for the power and thermal management (such as custom batteries, generators, or an air conditioning system) and limits the range and the payload of the vehicle. Thus, a low-power system simplifies the design and field operation.

Both QCL sensors consume much more power than the laser-based LI-7700 as shown in Table 1. The LI-7700 used custom electronics/microprocessor inherent to the instrument to control the sensor and reduce the power consumption, whereas the two QCL sensors used a general data acquisition board (National Instruments, NI-DAQ USB 6251) with a separate, dedicated computer. Another important difference was the higher power consumption of QCLs compared to vertical cavity surface emitting lasers (VCSELs). The LI-7700 used a 1.65 μm VCSEL that consumed ~10 mW of electrical power to produce ~1 mW of optical power (plus an additional W of power for laser thermal control). In contrast, the QCLs needed much higher electrical power (4–8 W) to produce 10–100 s mW optical power. Several more watts of the electrical power were also needed for laser temperature control by a thermoelectric cooler (TEC). In addition, the MCT (mercury cadmium telluride) detectors (Intelligent Material Solutions Inc. and Teledyne Judson Technologies)

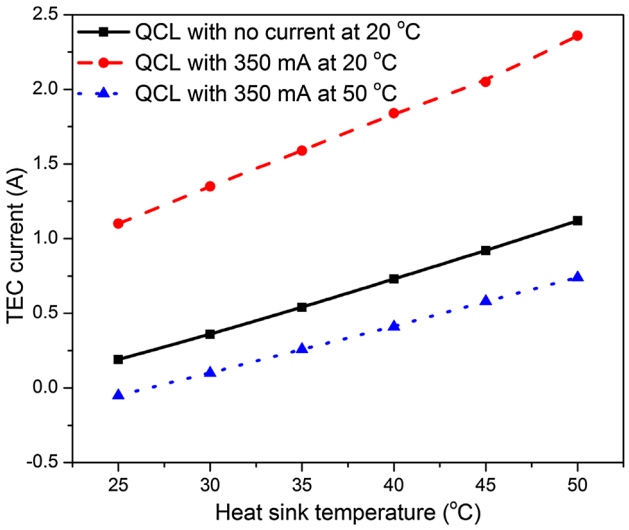

Fig. 4 QCL TEC current versus heat sink temperature at three different conditions

for the mid-IR detection in two QCL sensors operated at −50 °C for optimal sensitivity, which added another few watts (1–3 W) of the electrical power for the active cooling.

As a result of the QCLs' high power consumption, another field challenge was to maintain QCL's thermal stability in the field where ambient air temperatures reached 40 °C and laser case temperatures even higher when under the direct exposure of the sun and heat radiated from the car surface on summer days. One solution to this challenge was the use of specially selected QCLs ('hot' lasers) that probed the desired wavelength at an elevated temperature (40 °C or above). Figure 4 shows an example of the laser TEC currents needed at the different QCL operating conditions. In this experiment, a 4.5 μm QCL (Corning Inc., USA) was mounted on top of a secondary plate to test the current draw at different sink temperatures and laser injection currents at ambient room temperatures. The three experimental conditions were as follows: maintaining the QCL at 20 °C but with no laser injection current, the QCL operating at 350 mA current and a temperature of 20 °C, and the QCL with a 350 mA current at 50 °C. Clearly, a 'hot' laser is easier to be thermally controlled in the ambient condition. In fact, because of the inefficiency of cooling over heating, it required more power to cool an unoperating laser to 20 °C at any heat sink temperature than one where the laser operated at 50 °C and 350 mA of current. In the mobile sensors, the QCLs were mounted and heat sinked to the entire aluminum sensor head, which in turn was connected to the mirror mount and Mo mirror. This configuration helped to dissipate the heat as well as heated the mirror slightly to prevent dew formation. Both QCLs used for the NH_3 and N_2O/CO sensors operated above 40 °C and resulted in thermally stable operation in the field with just passive heat sinking.

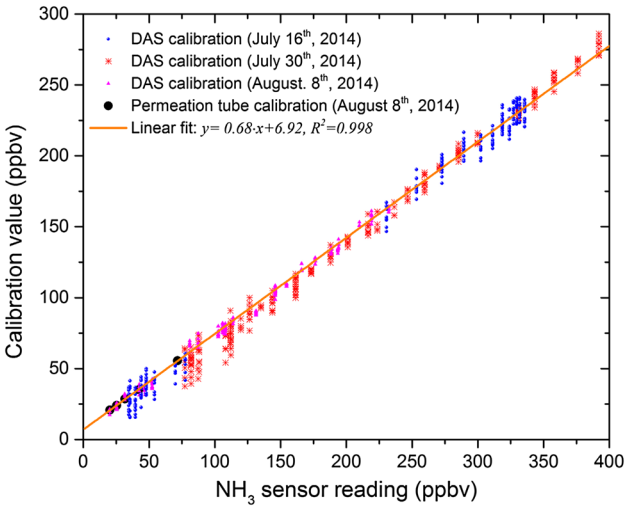

Fig. 5 Calibration of NH_3 sensor at different times. The x-axis is the raw data based upon dilution of a standard prior to using direct absorption spectroscopy

2.5 Calibration

For all of the open-path sensors, calibrations were performed by enclosing the sensor and flowing a gas standard (or some diluted amount of it) into the enclosure. However, it was too difficult to perform such calibrations on-road with the sensors mounted on top of the vehicle. Therefore, it was necessary to take the sensor off the vehicle to perform the calibrations before and after on-road measurements to ensure the consistency of the calibrations. CO_2, CH_4, N_2O, and CO were calibrated with a NOAA ESRL gas standard (393.444 ± 0.003 ppmv CO_2; 1871.3 ± 0.1 ppbv CH_4; 138.5 ± 1 ppbv CO; and 325.81 ± 0.15 ppbv N_2O). Note that for mixing ratios approximately greater than twice the ambient background, certified gas standards of accuracies of ±5 % were used. H_2O was calibrated with a dew point generator (LI-610 from LI-COR). The calibration of NH_3 was challenging due to its ability to adsorb on and desorb off calibration surfaces and gas handling lines. To calibrate the open-path NH_3 sensor in the laboratory, a large hermetically sealed aluminum enclosure (1.5 × 0.3 × 0.4 m) was placed over the entire sensor. The large surface area of the enclosure created sampling bias from surface effects. Indeed, readings on average were 68 % lower than those predicted from dilutions of a 5 ppmv NH_3 standard (Air Liquide).

To address the problems of calibrating NH_3, direct absorption spectroscopy (DAS) was used to derive accurate measurements of the gas phase NH_3 concentrations inside the calibration enclosure, as opposed to solely using the predicted values from the gas standard [14]. Spectroscopic parameters to deduce absolute concentrations were obtained from Sun et al. [26]. Dry nitrogen (N_2) was flown into the chamber, and a saturated citric acid solution was applied to the calibration chamber surfaces to scrub residual NH_3 off the surface of the calibration enclosure for the 'zero.' Figure 5 shows an example of the field calibration for the NH_3 sensor on three different days of a field campaign. On August 8, a calibration of NH_3 with a temperature-controlled NH_3 permeation tube from NOAA ESRL/Chemical Sciences Division [Kin-tek, La Marque, Texas, USA; 27] was also conducted as a secondary check on the direct absorption measurements and to validate the lower range of NH_3 mixing ratios. The field calibrations and spectroscopic data showed that the measurement accuracy of NH_3 was ±10 %.

2.6 Impact of self-emission and sensor separations

The exhaust from the vehicle itself can easily contaminate the ambient air samples and influence the measurement of the sensors on mobile platforms. In a closed-path mobile system, the exhaust from a generator is another possible source for sample contamination. Previously, closed-path mobile systems have tried to minimize self-emission contamination by positioning the sample inlet in a certain orientation relative to the exhaust pipes [3] or installing an exhaust-removal system [9]. The open-path design, however, inherently has no control on what air to sample. As a result, the sensors do measure the emissions from the host vehicles in certain situations such as backing up or being parked with the engine on. Figure 6 shows simple 2D flow simulations around a Chevy Impala vehicle from both the forward and backward directions (with videos provided as supplemental material). The simulation was done with Flowsquare Ver. 3.1 by using a computational fluid dynamics model [28]. In the simulation, the black bar on top of a 2013 Chevy Impala represents the sensors. The air flow was set to a speed of 10 m s^{-1} or a 36 km hr^{-1} vehicle speed in a calm atmosphere. When driving in the forward direction or having a strong headwind, the simulations suggested that the sensor heads would sample gas from the front of the vehicle and thus the self-emission would not contaminate the air sample measured by the sensors. When driving in the backward direction or having a strong tailwind, the air sample measured by the sensors would be dominated by self-emissions. Although this 2D simulation helps to visualize the air flow around the vehicle, it does not take into account the wind velocity perpendicular to the car direction nor does it account for the fact that emissions are not on the centerline of the vehicle. In general, a sufficient headwind is needed to push the self exhaust away from sensor heads and this has been confirmed in the field when driving in isolated areas where only the self-emissions were sources [as evidenced by CO measurements; 15]. While each campaign is specific to weather conditions, a general method is to set a threshold for CO enhancements above the background.

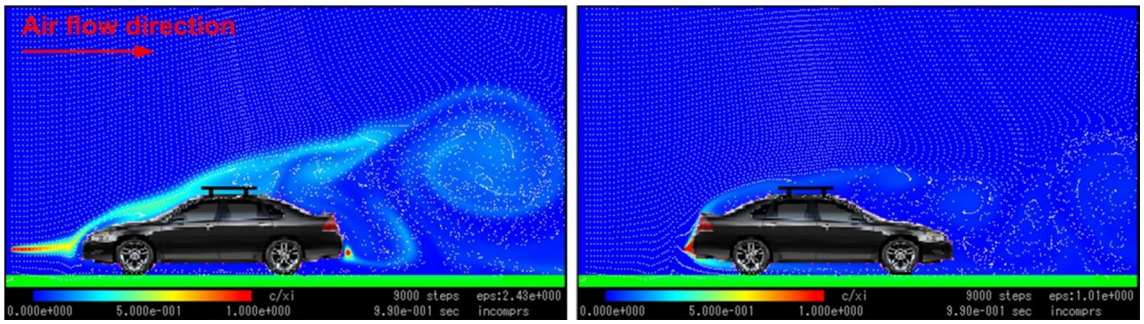

Fig. 6 2D air flow simulations for 2013 Chevy Impala. The *black bar* on the top of the vehicle represents the roof rack mount with sensor heads. *White dots* are a pictorial representation of the air. The *color map* represents the strength of emission from point sources. (*left*) Air flow from head to tail with one point source at front of the vehicle and the other one at the tailpipe; (*right*) air flow from tail to head with one point source at the tailpipe

Fig. 7 Mobile platform with an elevated frame

In a more recent design, however, the two aluminum breadboards were replaced with an aluminum structural frame to raise the height of all the sensors by 1.5 m above the roof of the vehicle as shown in Fig. 7. In the situations as is shown in the right frame of Fig. 6, a higher location would help to reduce the influence from tailpipe emissions. In the practical data analysis of the measured data, a more sophisticated filter based on a combination of wind speed, wind direction, vehicle speed, and vehicle bearing can be used to remove any potential contaminated measurements [15]. The ultimate solution to the self contamination problem would be to use a zero emission vehicle such as an electric vehicle. Because of the high flexibility of the low-power, open-path mobile sensing platform, there is no technical problem to install it on an electric vehicle. The limitation would be the availability of such an electric vehicle, its limited driving range and duration, and how a 200 W power draw and associated sensor drag may reduce its practical range even further.

Another concern of the mobile laboratory is whether the four open-path sensor heads measure the same gas sample. Unlike using a single gas sample inlet in the closed-path sensing platforms, the open-path sensors each have their own sample cells. The four optical sample cells were with their optical axes in parallel and within 45 cm of one another on top of the car as shown in Fig. 1. In the atmospheric boundary layer, gas molecules are mixed predominantly by turbulence [29]. In order for all four sensors to measure the same gas sample, the eddies created by the turbulence need to have negligible change as they advect past the entire sensor system. More formally, the measure of the intensity of the turbulence requirement is as follows:

$$\sigma_{\mathrm{M}} < 0.5\mathrm{M} \tag{1}$$

where σ_{M} is the standard deviation of the horizontal wind speed and M is the wind speed [30]. As the vehicle moves on-road, the effective horizontal wind speed M is the sum of the actual wind speed and the vehicle velocity vectors. The amplitude of M is usually from 5 m s^{-1} to 30 m s^{-1}, which is significantly larger than the value of σ_{M} (generally <1 m s^{-1}). Thus, the mobile sensing platform in most driving situations satisfies the condition for the Taylor's hypothesis [29]. In other words, the turbulence can be considered to be frozen as it advects past the sensors. For a stationary measurement, Eq. 1 also needs to be fulfilled for all sensors to measure the same gas sample. The correlation analyses between the gas molecules measured from different sensors can also be used as evidence for the measurements of the same gas sample as shown in the supporting information from Sun et al. [15]. The influence of the small spatial separations between the four sensors to the measurements can be ignored under the satisfaction of Taylor's hypothesis.

3 Field measurements and results

The mobile platform performed the spatial surveys of greenhouse gases and air pollutant emissions in five major

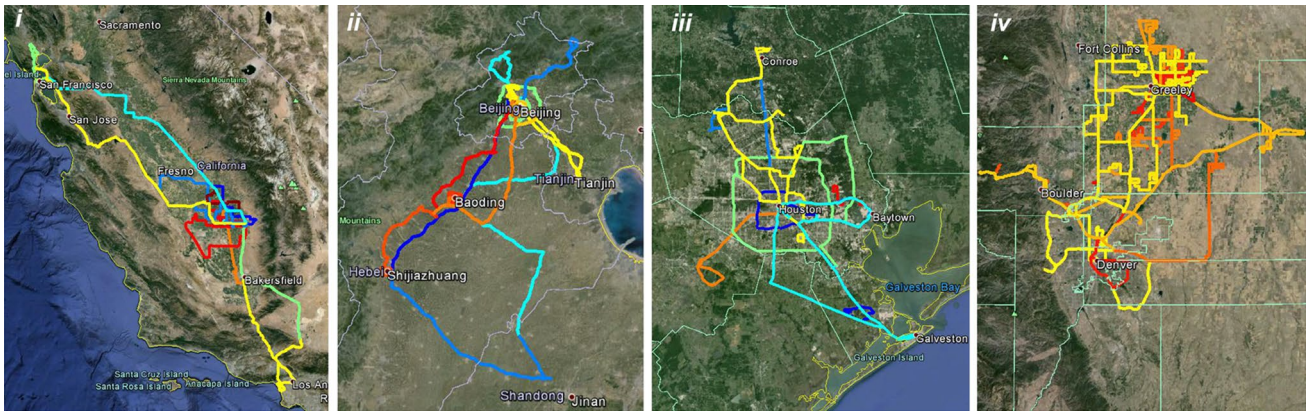

Fig. 8 Driven routes for different field campaigns: **i** DISCOVER-AQ in California **ii** CAREBEIJING **iii** DISCOVER-AQ in Houston **iv** DISCOVER-AQ in Colorado

field campaigns including three NASA DISCOVER-AQ (Deriving Information on Surface conditions from Column and Vertically Resolved Observations Relevant to Air Quality) field campaigns in California (January–February 2013), Houston (September 2013), and Colorado (July–August 2014) [31], and two CAREBEIJING (Campaigns of Air Quality Research in Beijing and Surrounding Regions) field campaigns [5] in Beijing and the surrounding Northern China Plain (NCP) during June 2013 and June 2014. Figure 8 shows the spatial coverage of the mobile platform in select campaigns with different colors illustrating measurements conducted on different days. Note that numerous paths overlap in these figures. A total of more than 400 h of on-road measurements were conducted that covered more than 18,000 km in distance. In this section, the measurement results from the CAREBEIJING field campaigns are shown as representative examples.

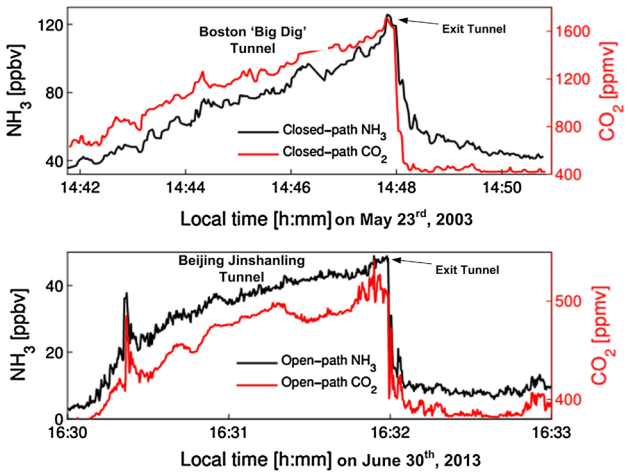

Fig. 9 Sensor response comparison between closed-path [4] and open-path tunnel measurements

3.1 On-road sensor response and stability

One of the major advantages for open-path sensing is its fast response to large changes of gas sample concentrations, particularly for the sticky gas molecules like NH_3. Figure 9 shows a comparison between two tunnel measurements for a closed-path mobile laboratory and the open-path mobile sensing platform. The top frame was measured in the Boston 'Big Dig' tunnel with Aerodyne Research's mobile laboratory on May 23, 2003 [4]. The bottom frame was measured in the Jinshanling tunnel by the open-path mobile platform on June 30, 2013, in China. Both the NH_3 and CO_2 mixing ratios increased because they derived from the same source, namely vehicle exhaust [15]. Thus, strong correlations are expected between NH_3 and CO_2 mixing ratios inside and near the tunnels. In both cases, measured CO_2 and NH_3 mixing ratios increased inside the tunnels and decreased after the tunnel exits. However, NH_3 measured by the closed-path system decayed much slower when compared to the non-sticky CO_2 measured at the same time. In contrast, NH_3 measured by the open-path system showed no delay compared to the CO_2 measurements. The open-path sensors show much faster responses to large changes in concentrations for gas molecules that show high affinities to surfaces when compared to closed-path sensors.

The on-road stability of open-path sensors was examined using the inline reference signal during the measurements. In both QCL sensors, gas reference cells have been installed in-line with the multipass optical cells to provide reference absorption signals [13, 14, 26]. The NH_3 sensor used a low-pressure ethylene (C_2H_4) gas reference cell [50 hPa; 14], whereas the N_2O/CO sensor used a low-pressure acetylene (C_2H_2) gas reference cell [133 hPa; 13]. In the NH_3 sensor, the 8th harmonic of C_2H_4 was used to isolate the reference signal from ambient NH_3 signal [14, 26]. Although the

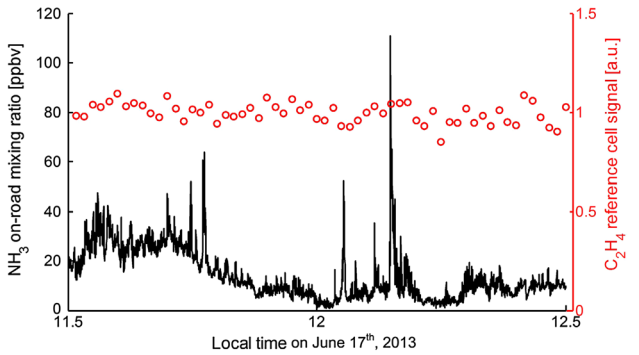

Fig. 10 Time series of the measured NH_3 and inline reference C_2H_4 signals. Note that the inline reference signal is derived from the intrinsically noisier 8th harmonic and provides a metric of drift/stability on timescales of hours to days

high harmonics were inherently much nosier than the 2nd harmonic signals, they can still provide a measure of the system stability at longer timescales. Figure 10 shows the time series of the measured NH_3 and inline reference signals during an hour drive from Beijing to Shijiazhuang, China, on June 17, 2013. The 1 min averaged 8th harmonic signal of C_2H_4 is plotted together with the 1 Hz NH_3 concentrations on-road. Although ambient NH_3 mixing ratios varied by over two orders of magnitude, the coefficient of variation (standard deviation divided by mean) for the C_2H_4 reference cell signal was 5.1 % during this part of the drive. Note that short-term stability (<10 min) has already been demonstrated for these sensors previously. Instead, it is the long-term stability (hours to days) in a changing field environment that is a problem for most field-based sensors, and the in-line reference cell provided a means to address stability at these times scales between calibrations.

3.2 Spatial and temporal mapping of gas concentrations

Megacities like Beijing have various anthropogenic activities resulting in greenhouse gas and air pollutant emissions that influence the regional air quality and the global climate change. A vehicle-based mobile sensing platform provides high spatial and temporal measurements of important trace gases emitted from heterogeneous anthropogenic emissions. Figure 11 shows maps of Beijing overlaid with measured CH_4 and NH_3 concentrations, respectively. The 10-Hz CH_4 and NH_3 measured on different days were averaged spatially to achieve a 100 m resolution for the illustration of the spatial coverage. The mobile platform captured various CH_4 and NH_3 emission hot spots as well as more typical background values around the city. The observations showed a high spatial heterogeneity of both CH_4 and NH_3 mixing ratios that would be difficult to capture by stationary monitoring sites such as the one located at Peking University.

The mobile platform also performed measurements at the same locations to discern diurnal trends of key pollutants. Figure 12 shows the measured CO mixing ratios on the Fourth Ring Road of Beijing at different times of the day. The measured CO mixing ratios show a temporal evolution strongly controlled by daily traffic patterns with a morning and evening rush hour clearly evident. In addition, spatial patterns are also observed such as along the northeast part of the ring road where mixing ratios are the highest, largely due to traffic congestion in this case.

3.3 Identify and characterize emission sources

There are many different types of emission sources in an urban city and its surrounding area. It is usually difficult to directly identify which type of emission source causes

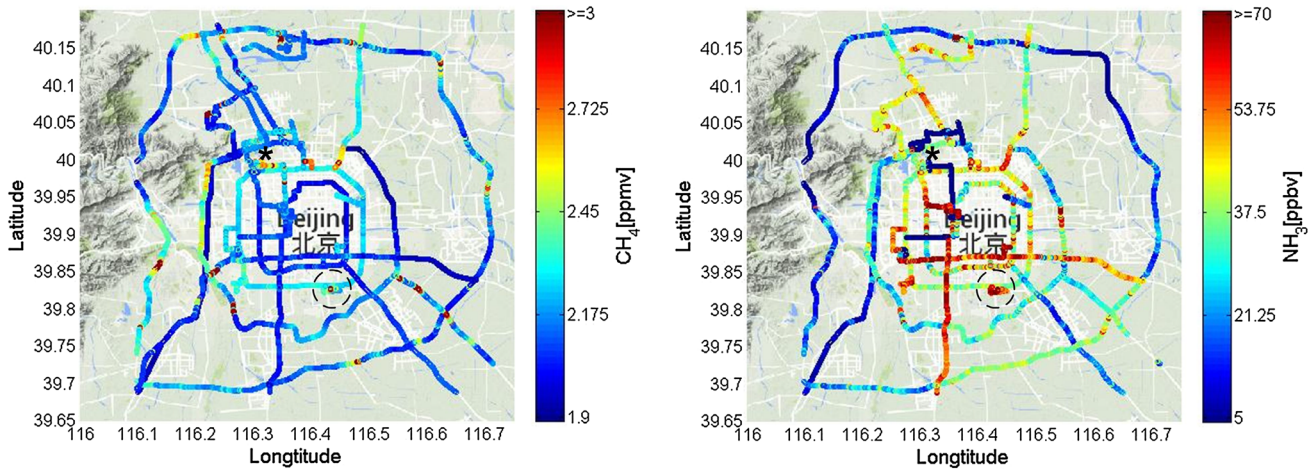

Fig. 11 Map of the measured CH_4 and NH_3 concentrations in Beijing; a *black dash circle* encloses a wastewater treatment facility in the city; a *black star* sign marks the location of stationary site at Peking University

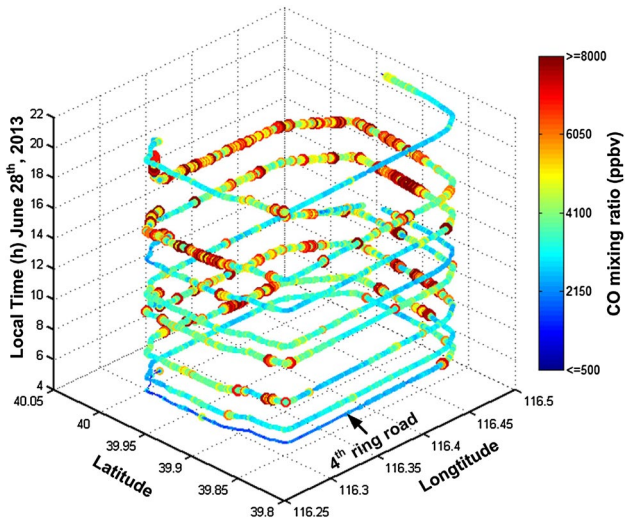

Fig. 12 Measured CO mixing ratios from the continuous mapping on the fourth ring road in Beijing on June 28, 2013

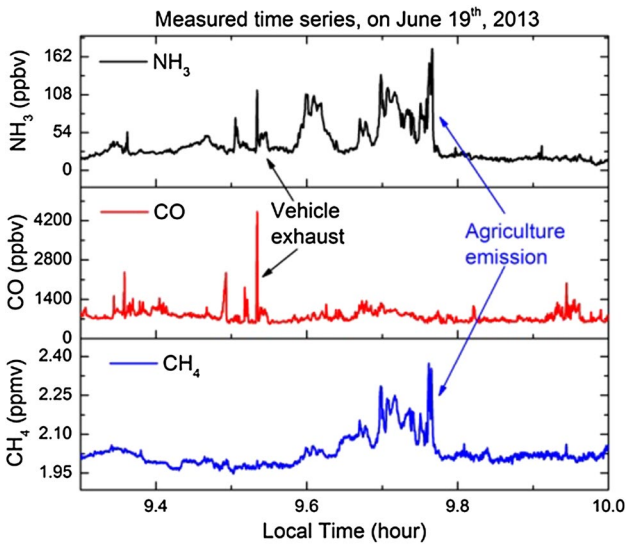

Fig. 13 Time series of NH_3, CO, and CH_4 from different emission sources

the increase in a trace gas with a single gas measurement. One important objective for the mobile sensing platform is to fingerprint individual sources. Simultaneous detection of CO_2, CH_4, N_2O, CO, and NH_3 offers great advantages in identifying different emission sources and understanding their emission signatures. Figure 13 shows a time series of NH_3, CO, and CH_4 mixing ratios during CAREBEIJING. There exist many correlated enhancement features which can help to deduce sources of NH_3, for example. Carbon monoxide is an excellent tracer of the fossil fuel combustion. Correlations of CO and NH_3 suggest emissions from vehicle exhaust as NH_3 is emitted from three-way catalytic converters [15]. Correlations of NH_3 and CH_4 with a low CO level indicate emissions of a biogenic agricultural source. The multi-gas observation not only helps to identify different emission sources but also helps to quantify the emission signatures. The NH_3 emission factors from the vehicles can be derived as the ratio of the enhanced NH_3 concentrations and the enhanced CO/CO_2 concentrations for the vehicle emission analyses. To this end, on-road vehicle NH_3 emissions have been characterized with a dependence on both the road gradients and the vehicle-driving conditions [15]. In an analogous study to the vehicle emissions, the NH_3 and CH_4 emissions of the dairy farms have also been studied with the measurements from the DISCOVER-AQ California field campaign [16].

The combination of the spatial information from the GPS and the different mixing ratios helps to locate the emission sources in complicated environments. Figure 14 shows a satellite image of a wastewater treatment facility circled in Fig. 11. The figure is overlaid with the measured 10 Hz CH_4, NH_3, and N_2O concentrations. The emissions from the wastewater treatment facility are complicated and related to different treatment processes. Under an east wind, the mobile observations showed elevated levels of CH_4, NH_3, and N_2O on the downwind side of the wastewater treatment facility. In addition, N_2O itself showed strong increases on the upwind side. The cause of the upwind increase was visually identified as emissions from a water discharge into a nearby river (white circle on the map). In this case, emissions from the discharged water after treatment had high N_2O but low CH_4 and NH_3 emissions. This example demonstrates the capability of the mobile sensing platform to pinpoint and characterize different emission sources with high spatial resolution.

4 Conclusions and future outlook

In this paper, the development of a mobile sensing platform formed with multiple open-path sensors has been demonstrated. The advantage for using an open-path design for sensors is low power consumption, low mass, fewer sampling artifacts, and fast sampling response. The mobile system can also be easily installed on common passenger vehicles for field studies. The mobile sensor system consumes only 200 W with a mass of 35 kg—a significant improvement for portable, long-term mobile sensing compared with large closed-path mobile laboratory vans. It measures six different gas molecules including all major greenhouse gases and two important air pollutants. The mobile sensing platform has been installed on top of the common passenger vehicles for multiple field campaigns in both the USA

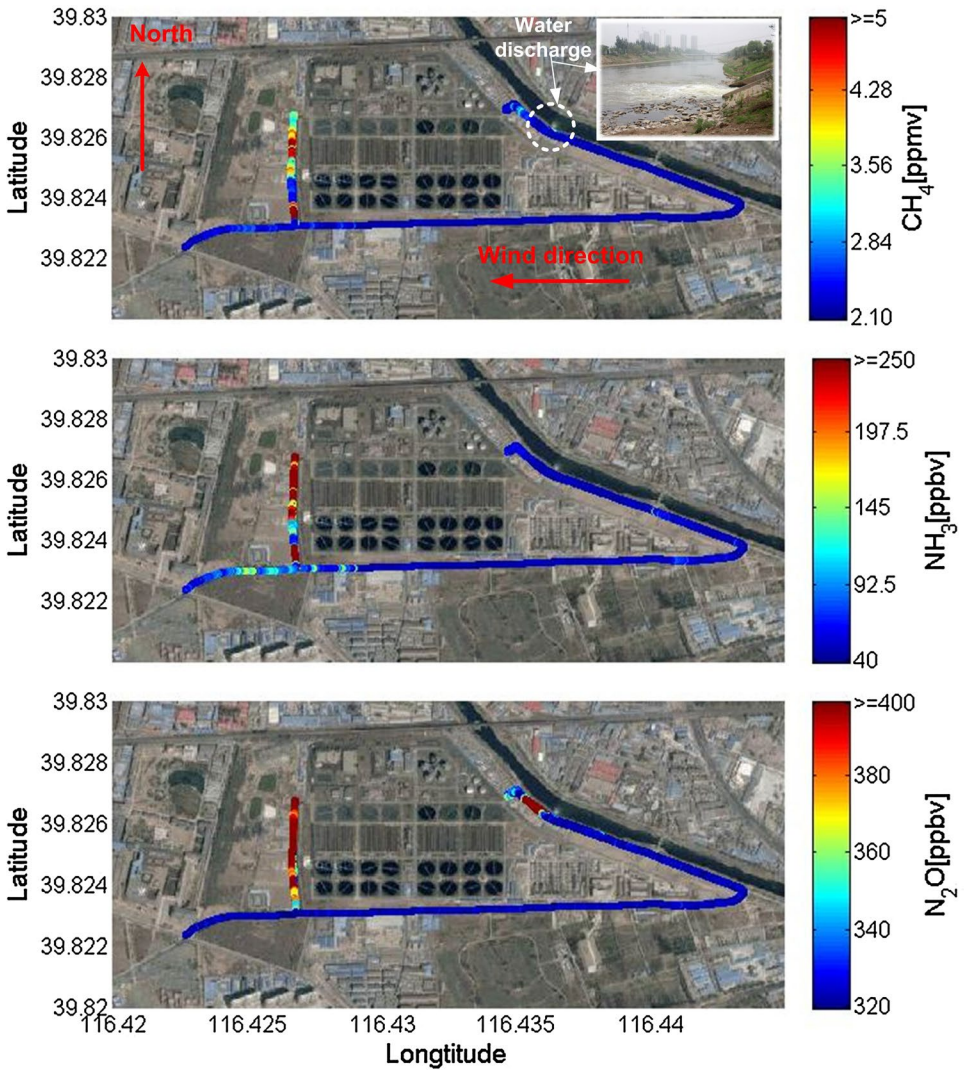

Fig. 14 CH_4, NH_3, and N_2O concentrations measured near a wastewater treatment facility in Beijing. The *white dashed circle* in the top frame shows the location of a water discharge into a nearby river as shown in the *inset photograph*

and China. The field observations with this mobile sensing platform have shown its advantages in quickly mapping a large spatial area with the capability to identify and quantify the different emission sources.

For future system development, a shared optical cell would reduce the overall size and mass of the platform and provide a common measurement length scale (optical base path) among all species. More experiments are needed to verify sensor precision and calibration while driving. Waterproofing the sensors is also needed. New sensors to measure gases such as ethane (C_2H_6) and nitric oxide (NO) are being developed to expand the measurement capabilities. Finally, while the mobile sensing platform is a low power and highly flexible unit, there remain challenges in optimizing the sampling strategy for mobile-based measurements in order to quantify local emissions accurately.

Acknowledgments The authors acknowledge the following people associated with the mobile platform development and deployment including James Smith, Claire Gmachl, Elie Bou-Zeid, and Denise Mauzerall at Princeton University, Tong Zhu at Peking University, Barry Lefer at University of Houston, Robert Griffin at Rice University, Jim Crawford at NASA Langley Research Center, the NASA DISCOVER-AQ science team, Andrew Neuman and Thomas Ryerson at NOAA ESRL Chemical Sciences Division for calibrations with their NH_3 permeation source, Dayle McDermitt from LICOR Biosceiences, and Yan Zhang from Scinovation. The research is supported by Princeton University, the National Geographic Air and Water Conservation Fund, NSF Center for Mid-Infrared Technologies for Health and the Environment (MIRTHE, NSF-ERC) under Grant No. EEC-0540832. Special thanks to the support and helpful discussions with LI-COR Environmental division and for providing a set of LICOR sensors for the mobile laboratory. K. Sun acknowledges support by NASA Earth and Space Science Fellowship (NN12AN64H). D. J. Miller acknowledges support by the National Science Foundation Graduate Research Fellowship (DGE-0646086). We thank two anonymous reviewers for very helpful feedback and comments on the manuscript.

References

1. H.L. Brantley, G.S.W. Hagler, E.S. Kimbrough, R.W. Williams, S. Mukerjee, L.M. Neas, Mobile air monitoring data-processing strategies and effects on spatial air pollution trends. Atmos. Meas. Tech **7**(7), 2169–2183 (2014)
2. M. Zavala, S.C. Herndon, R.S. Slott, E.J. Dunlea, L.C. Marr, J.H. Shorter, M. Zahniser, W.B. Knighton, T.M. Rogers, C.E. Kolb, L.T. Molina, M.J. Molina, Characterization of on-road vehicle emissions in the Mexico City Metropolitan Area using a mobile laboratory in chase and fleet average measurement modes during the MCMA-2003 field campaign. Atmos. Chem. Phys. **6**(3), 4689–4725 (2006)
3. C.E. Kolb, S.C. Herndon, J.B. McManus, J.H. Shorter, M.S. Zahniser, D.D. Nelson, J.T. Jayne, M.R. Canagaratna, D.R. Worsnop, Mobile laboratory with rapid response instruments for real-time measurements of urban and regional trace gas and particulate distributions and emission source characteristics. Environ. Sci. Technol. **38**(21), 5694–5703 (2004)
4. S.C. Herndon, J.T. Jayne, M.S. Zahniser, D.R. Worsnop, B. Knighton, E. Alwine, B.K. Lamb, M. Zavala, D.D. Nelson, J.B. McManus, J.H. Shorter, M.R. Canagaratna, T.B. Onasch, C.E. Kolb, Characterization of urban pollutant emission fluxes and ambient concentration distributions using a mobile laboratory with rapid response instrumentation. Faraday Discuss. **130**, 327 (2005)
5. M. Wang, T. Zhu, J. Zheng, R.Y. Zhang, S.Q. Zhang, X.X. Xie, Y.Q. Han, Y. Li, Use of a mobile laboratory to evaluate changes in on-road air pollutants during the Beijing 2008 Summer Olympics. Atmos. Chem. Phys. **9**(3), 12857–12898 (2009)
6. P. Farrell, D. Culling, I. Leifer, Transcontinental methane measurements. Part 1. A mobile surface platform for source investigations. Atmos. Environ. **74**, 422–431 (2013)
7. L.T. Padró-Martínez, A.P. Patton, J.B. Trull, W. Zamore, D. Brugge, J.L. Durant, Mobile monitoring of particle number concentration and other traffic-related air pollutants in a near-highway neighborhood over the course of a year. Atmos. Environ. **1994**(61), 253–264 (2012)
8. N. Bukowiecki, J. Dommen, A.S.H. Prévôt, R. Richter, E. Weingartner, U. Baltensperger, A mobile pollutant measurement laboratory—measuring gas phase and aerosol ambient concentrations with high spatial and temporal resolution. Atmos. Environ. **36**(36–37), 5569–5579 (2002)
9. F. Drewnick, T. Böttger, S.-L. von der Weiden-Reinmüller, S.R. Zorn, T. Klimach, J. Schneider, S. Borrmann, Design of a mobile aerosol research laboratory and data processing tools for effective stationary and mobile field measurements. Atmos. Meas. Tech **5**(6), 1443–1457 (2012)
10. P. Werle, Diode-Laser sensors for in situ gas analysis, in *Laser in environmental and life sciences modern analytical methods*, ed. by P. Hering, J.P. Lay, S. Stry (Springer, Berlin, 2004), pp. 223–243
11. M.A. Zondlo, M.E. Paige, S.M. Massick, J.A. Silver, Vertical cavity laser hygrometer for the National Science Foundation Gulfstream-V aircraft. J. Geophys. Res. **115**(D20), D20309 (2010)
12. A. Khan, D. Schaefer, L. Tao, D.J. Miller, K. Sun, M.A. Zondlo, W.A. Harrison, B. Roscoe, D.J. Lary, Low power Greenhouse gas sensors for unmanned Aerial Vehicles. Remote Sens **4**(12), 1355–1368 (2012)
13. L. Tao, K. Sun, M.A. Khan, D.J. Miller, M.A. Zondlo, Compact and portable open-path sensor for simultaneous measurements of atmospheric N_2O and CO using a quantum cascade laser. Opt. Express **20**(27), 28106–28118 (2012)
14. D.J. Miller, K. Sun, L. Tao, M.A. Khan, M.A. Zondlo, Open-path, quantum cascade-laser-based sensor for high-resolution atmospheric ammonia measurements. Atmos. Meas. Tech **7**(1), 81–93 (2014)
15. K. Sun, L. Tao, D.J. Miller, M.A. Khan, M.A. Zondlo, On-road ammonia emissions characterized by mobile, open-path measurements. Environ. Sci. Technol. **48**(7), 3943–3950 (2014)
16. D.J. Miller, K. Sun, L. Tao, M.A. Zondlo, J.B. Nowak, Z. Liu, G. Diskin, G. Sachse, A. Beyersdorf, R. Ferrare, A.J. Scarino, Ammonia and methane dairy emission plumes in the San Joaquin Valley of California from individual feedlot to regional scales, to be submitted to J. Geophys. Res. Atmos. manuscript ID 2015JD023241 (2015)
17. D. McDermitt, G. Burba, L. Xu, T. Anderson, A. Komissarov, B. Riensche, J. Schedlbauer, G. Starr, D. Zona, W. Oechel, S. Oberbauer, S. Hastings, A new low-power, open-path instrument for measuring methane flux by eddy covariance. Appl. Phys. B **102**(2), 391–405 (2010)
18. LI-COR Biosceiences. LI-7500A Open Path CO2/H2O analyzer brochure, (Dec., 2014). Retrieved from http://www.licor.com/env/pdf/gas_analyzers/7500A/LI-7500A_brochure.pdf
19. J.M. Supplee, E.A. Whittaker, W. Lenth, Theoretical description of frequency-modulation and wavelength modulation spectroscopy. Appl. Opt. **33**(27), 6294–6302 (1994)
20. D. Belušić, D.H. Lenschow, N.J. Tapper, Performance of a mobile car platform for mean wind and turbulence measurements. Atmos. Meas. Tech **7**(6), 1825–1837 (2014)
21. D. Herriott, H. Kogelnik, R. Kompfner, Off-Axis Paths in Spherical Mirror Interferometers. Appl. Opt. **3**(4), 523 (1964)
22. J.A. Silver, Simple dense-pattern optical multipass cells. Appl. Opt. **44**(31), 6545 (2005)
23. J.B. Mcmanus, mirror resonators with twisted axes for laser spectroscopy. Appl. Opt. **46**(4), 472–482 (2007)
24. D.-Y. Song, R.W. Sprague, H.A. Macleod, M.R. Jacobson, Progress in the development of a durable silver-based high-reflectance coating for astronomical telescopes. Appl. Opt. **24**(8), 1164 (1985)
25. D.W. Rice, Atmospheric corrosion of Copper and Silver. J. Electrochem. Soc. **128**(2), 275 (1981)
26. K. Sun, L. Tao, D.J. Miller, M.A. Khan, M.A. Zondlo, Inline multi-harmonic calibration method for open-path atmospheric ammonia measurements. Appl. Phys. B **110**(2), 213–222 (2012)
27. J.B. Nowak, J.A. Neuman, K. Kozai, L.G. Huey, D.J. Tanner, J.S. Holloway, T.B. Ryerson, G.J. Frost, S.A. McKeen, F.C. Fehsenfeld, A chemical ionization mass spectrometry technique for airborne measurements of ammonia. J. Geophys. Res. **112**(D10), D10S02 (2007)
28. Y. Minamoto, Flowsquare 3.1b [Computer software], (Mar., 2014). Retrieved from http://flowsquare.com/
29. G.I. Taylor, The spectrum of turbulence. Proc. R. Soc. A Math. Phys Eng. Sci **164**(919), 476–490 (1938)
30. G.E. Willis, J.W. Deardorff, On the use of Taylor's translation hypothesis for diffusion in the mixed layer. Q. J. R. Meteorol. Soc. **102**(434), 817–822 (1976)
31. NASA, DISCOVER-AQ Mission, (Dec., 2014). Retrieved from http://www.nasa.gov/mission_pages/discover-aq/#.VE8lSmca9Es